

ChemComm

Accepted Manuscript



This article can be cited before page numbers have been issued, to do this please use: G. Han, Y. Wang, H. Li, Z. Yang and S. Pan, *Chem. Commun.*, 2019, DOI: 10.1039/C8CC10158B.



This is an Accepted Manuscript, which has been through the Royal Society of Chemistry peer review process and has been accepted for publication.

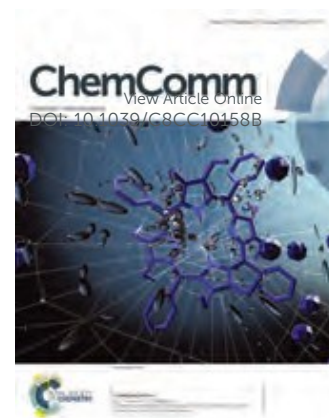
Accepted Manuscripts are published online shortly after acceptance, before technical editing, formatting and proof reading. Using this free service, authors can make their results available to the community, in citable form, before we publish the edited article. We will replace this Accepted Manuscript with the edited and formatted Advance Article as soon as it is available.

You can find more information about Accepted Manuscripts in the [author guidelines](#).

Please note that technical editing may introduce minor changes to the text and/or graphics, which may alter content. The journal's standard [Terms & Conditions](#) and the ethical guidelines, outlined in our [author and reviewer resource centre](#), still apply. In no event shall the Royal Society of Chemistry be held responsible for any errors or omissions in this Accepted Manuscript or any consequences arising from the use of any information it contains.

Chemical Communications

Guidelines for reviewers



ChemComm is a forum for urgent high quality communications from across the chemical sciences.

Communications in *ChemComm* should be preliminary accounts of **original and urgent work** of significance to a general chemistry audience. The 2017 Impact Factor for *ChemComm* is **6.290**.

Only work within the top 25% of the field in terms of quality and interest should be recommended for publication. Acceptance should only be recommended if the content is of such urgency and significant general interest that rapid publication will be advantageous to the progress of chemical research.

Routine and incremental work – however competently researched and reported – should not be recommended for publication.

Articles which rely excessively on supplementary information should not be recommended for publication.

Thank you very much for your assistance in evaluating this manuscript.

General Guidance

Reviewers have the responsibility to treat the manuscript as confidential. Please be aware of our [Ethical Guidelines](#), which contain full information on the responsibilities of reviewers and authors, and our [Refereeing Procedure and Policy](#).

Supporting information and characterisation of new compounds

Experimental information must be provided to enable other researchers to reproduce the work accurately. It is the responsibility of authors to provide fully convincing evidence for the homogeneity, purity and identity of all compounds they claim as new. This evidence is required to establish that the properties and constants reported are those of the compound with the new structure claimed.

Please assess the evidence presented in support of the claims made by the authors and comment on whether adequate supporting information has been provided to address the above. Further details on the requirements for characterisation criteria can be found [here](#).

When preparing your report, please:

- comment on the originality, significance, impact and scientific reliability of the work;
- state clearly whether you would like to see the article accepted or rejected and give detailed comments (with references, as appropriate) that will both help the Editor to make a decision on the article and the authors to improve it;
- it is the expectation that only work with two strong endorsements will be accepted for publication.

Please inform the Editor if:

- there is a conflict of interest;
- there is a significant part of the work which you are not able to referee with confidence;
- the work, or a significant part of the work, has previously been published;
- you believe the work, or a significant part of the work, is currently submitted elsewhere;
- the work represents part of an unduly fragmented investigation.

Submit your report at <http://mc.manuscriptcentral.com/chemcomm>

COMMUNICATION

A Lithium Difluorophosphate LiPO_2F_2 with a Neutral Polytetrahedral Microporous Architecture

Guopeng Han,^{a,b,†} Ying Wang,^{a,†} Hao Li,^{a,b} Zhihua Yang,^a and Shilie Pan^{*a}Received 00th January 20xx,
Accepted 00th January 20xx

DOI: 10.1039/x0xx00000x

www.rsc.org/

We present herein the first lithium difluorophosphate LiPO_2F_2 exhibiting a unique polytetrahedral microporous architecture. The unique fluorine coordination environments and interlaced $[\text{LiO}_2]^{3-}$ straight chains give rise to the neutral pore framework with 10-membered ring channel along the crystallographic *c* axis. A variety of measurements have been adopted to systemically characterize LiPO_2F_2 . This work will contribute to the structural and functional diversity of phosphate chemistry by the exploration of the fascinating difluorophosphates.

The immensely widespread application of phosphates is dependent on the very large number of different phosphate phases and the diverse structures.¹ Among the variety of phosphates investigated in recent years, the fluorine-containing phosphates have aroused particular interest in inorganic chemistry not only because of the novelty in their structures, but also owing to their various and pretty useful properties, such as electrolyte for ion batteries, stabilizers for chloroethylene polymers, catalysts for reactive lubricants, antibacterial used in dentifrice formulations, and timber preservatives.² As a prominent presentative, $\text{Na}_2\text{PO}_3\text{F}$ is a well-known fluorophosphate commonly used in toothpaste.³

Fluorophosphates, in which the fluorine atoms covalently connect with the phosphorus atoms, show additional compositional and structural diversity compared to orthophosphates. Very recently, it was proposed that the oxyfluoride $[\text{BO}_x\text{F}_{4-x}]$ and $[\text{PO}_x\text{F}_{4-x}]$ ($1 < x < 4$) species are superior material genomes to obtain excellent optical properties.⁴ These oxyfluoride species with large polarizability anisotropies, wide HOMO–LUMO gaps, and high

hyperpolarizabilities are beneficial for the deep-ultraviolet optical properties of borates or phosphates.

In particular, the difluorophosphate radical PO_2F_2 is preferred for deep-ultraviolet optical materials compared to other oxyfluoride tetrahedra. It is shown that difluorophosphates exhibit larger birefringence and band gaps than monofluorophosphates and orthophosphates.^{4d} Besides, difluorophosphates were also studied as promising electrolyte salt or as electrolyte salt additive for Li/Na ion batteries.⁵ Therefore, difluorophosphates are one of the most fascinating system for searching new functional materials. However, the crystal growth of difluorophosphates with high quality single crystal is difficult because of their rigorous growth conditions and relatively poor thermal stability. As yet, only four alkali / alkaline earth / ammonium difluorophosphates with single crystal diffraction data have been reported, *i.e.* KPO_2F_2 ,⁶ RbPO_2F_2 ,⁷ CsPO_2F_2 ,⁸ and $\text{NH}_4\text{PO}_2\text{F}_2$.⁹ In this contribution, we present the first lithium difluorophosphate LiPO_2F_2 exhibiting a unique microporous architecture and improved optical properties. The colourless block-shaped crystals with centimeter-size were obtained (Figure S1, ESI).

The LiPO_2F_2 crystals were prepared by hydrothermal method using LiF, P_2O_5 , and HPF_6 as the raw materials. The crystal structure of LiPO_2F_2 was well-defined on the basis of single crystal diffraction data. The purity of the prepared sample was checked by powder X-ray diffraction (XRD) technique, which is consistent with the theoretical pattern from the single-crystal diffraction data (Figure S3, ESI). Details of the crystallographic data and structural refinements are provided in Table S1 in the ESI. The existence of fluorine and the P–F bonds was confirmed by elemental analysis (Figure S4, ESI), and IR spectroscopy, and the sites of F and O atoms were reasonably assigned by the bond valence sums (BVS) calculation.¹⁰

LiPO_2F_2 crystallizes in the monoclinic space group $C2/c$. There are twelve crystallographically different atoms in the asymmetric unit, including two Li atoms, two P atoms, four O atoms, and four F atoms (Figure S5, ESI). The Li and P atoms are all in tetrahedral coordination environments with O or F forming the LiO_4 and PO_2F_2 species, respectively. All O atoms are three-coordinated with two adjacent Li atoms and one adjacent P atom, and the F atoms are terminally bonded to one P atom. The PO_2F_2 tetrahedra are isolated from each

^a G. Han, Dr. Y. Wang, H. Li, Prof. Z. Yang, Prof. S. Pan, CAS Key Laboratory of Functional Materials and Devices for Special Environments, Xinjiang Technical Institute of Physics & Chemistry, CAS; Xinjiang Key Laboratory of Electronic Information Materials and Devices, 40-1 South Beijing Road, Urumqi 830011, China. Email: slpan@ms.xjb.ac.cn

^b G. Han and H. Li. Center of Materials Science and Optoelectronics Engineering, University of Chinese Academy of Sciences, Beijing 100049, China

[†] These authors contributed equally to this work.

Electronic Supplementary Information (ESI) available: Cif, synthesis, experimental detail, structural refinement and crystal data, EDX, transmittance spectrum, band structure, DOS, calculated refractive index. See DOI: 10.1039/x0xx00000x

other, while each LiO_4 tetrahedra are edge-shared with two adjacent LiO_4 tetrahedra forming infinite one-dimensional (1D) straight chains $[\text{LiO}_2]^{3-}$. The PO_2F_2 anion shows a distorted tetrahedral geometry with P-O bond lengths varying between 1.462(2) and 1.469(2) Å and P-F bond lengths ranging from 1.497(3) to 1.515(2) Å. The bond angle ranges of O-P-O, F-P-O, F-P-F in PO_2F_2 are 118.95(15)-121.67(18)°, 108.31(15)-109.67(15)°, and 99.2(3)-100.4(2)°, respectively. Since the PO_2F_2 units are isolated, the distortion of the bond angles from ideal tetrahedral value could be explained in terms of the valence-shell electron repulsion theory.¹¹ The LiO_4 units have these interatomic dimensions: Li-O bond lengths 1.910(5)-1.973(5) Å and O-Li-O bond angles 91.1(2)-131.6(3)°. The significant deviations from the ideal tetrahedral angle are mainly caused by two bridging O atoms among the Li atoms.

It is interesting to note that LiPO_2F_2 exhibits infinite $[\text{LiO}_2]^{3-}$ straight chains in two different directions (Figures 1c, 1d), which is the first example in all fluorophosphates. The two types of $[\text{LiO}_2]^{3-}$ chains stack alternately along the crystallographic *c* axis, which are further polymerized with the PO_2F_2 tetrahedra by corner-sharing common O atoms forming a 3D microporous framework. The unique 3D framework affords a 10-membered ring channel along the [001] direction (Figure 1e). Topologically, the LiO_4 and PO_2F_2 tetrahedra could be regarded as 6-connected and 4-connected nodes, respectively. Thus, the LiPO_2F_2 architecture could therefore be reduced to a topological $4,4,4,6,6\text{-}c$ 5-nodal net with a point symbol of $\{3^2.4.5^2.6\}\{3^2.5.6^2.7\}\{3^4.4^2.5^2.6^3.7^3.8\}\{3^4.4^3.5^4.6^4\}$ (Figure 2).

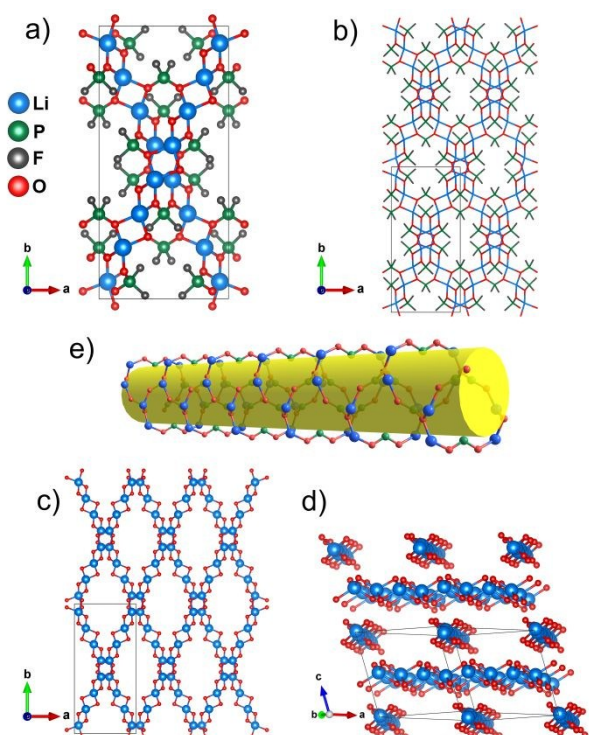


Figure 1. a) Projection of the LiPO_2F_2 structure and b) microporous architecture on the *ab* plane. Figures 1c and 1d present the interlaced $[\text{LiO}_2]^{3-}$ chains viewing along [001] and its perpendicular direction, respectively. e) The 10-membered ring channel along the [001] direction. The unit cells are indicated by the black boxes.

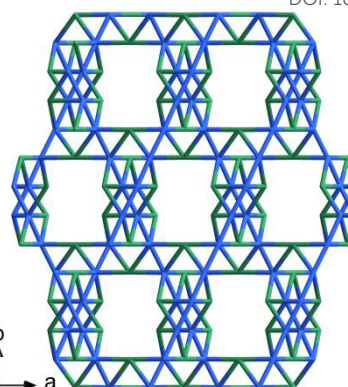


Figure 2. The topological structure of LiPO_2F_2 .

There are two key factors affecting the formation of the unique microporous architectures. Firstly, fluorine plays an important role. Different from bridging O atoms, all F atoms in LiPO_2F_2 are terminally bonded to the P atom, which cut off the dense 3D -O-Li/P-O- framework and create a pore framework, and the F atoms are located at the inner surface of the channels. Secondly, the interlaced $[\text{LiO}_2]^{3-}$ chains are another important factor to support the basic microporous architecture of LiPO_2F_2 (Figures 1c and 1d). The ammonium, potassium, rubidium, and cesium difluorophosphates are isomorphous (Orthorhombic, *Pnma*) with the barium sulphate structure type, and they do not share any structural similarity with LiPO_2F_2 . The cations certainly influence the backbone geometry of the structures mentioned above.¹² Besides, although the ClO_4 and SO_3F ions are isoelectronic with PO_2F_2 , the structures of LiClO_4 ¹³ and LiSO_3F ¹⁴ are also very different from that of LiPO_2F_2 (Figures S6, S7, ESI).

The microporous architecture of LiPO_2F_2 share similar features with zeolite aluminophosphates - one of the most widely known molecular sieves.¹⁵ They are all neutral polytetrahedral frameworks, which usually exhibit less affinity for H_2O than the anionic zeolite frameworks caused by the absence of the dipole interaction between the electrostatic fields of the anionic framework and the extra-framework cations. Owing to the novel structure of LiPO_2F_2 , some interesting properties, such as ionic conductivities, adsorptive and catalytic applications could be foreseen. For block LiPO_2F_2 crystal, a specific surface area of $38.6 \text{ m}^2\text{g}^{-1}$ has been determined by N_2 adsorption/desorption experiments. Typical isotherms and pore size distribution are shown in Figure S8 in the ESI. It is worth mentioning that the Brunauer – Emmett – Teller (BET) surface area of LiPO_2F_2 is much larger than that of $\text{K}_3\text{B}_6\text{O}_{10}\text{Br}$ nanoparticles ($0.05 \text{ m}^2\text{g}^{-1}$) and comparable to that of P25 TiO_2 ($58 \text{ m}^2\text{g}^{-1}$).¹⁶

Owing to the characteristic vibration bands in terms of intensity and frequency, the coordination geometry of phosphorus can be detected by IR spectrum. Figure 3 represents the calculated and experimental bands of LiPO_2F_2 , which are roughly consistent with each other. The strong vibration bands between $1400\text{-}800 \text{ cm}^{-1}$ mainly originate from stretching modes of tetrahedrally surrounded phosphorus (PO_2F_2). More narrowly, the bands observed at 1273,

1163 cm^{-1} are designated as the asymmetric and symmetric stretching of P-O bonds, respectively. The bands at 934, 887 cm^{-1} are assigned to the asymmetric and symmetric stretching of P-F bonds, respectively. It is interesting to note that the title compound also shows the strong vibration bands in the lower frequency region (700–400 cm^{-1}), which are predominant due to the bending and rocking modes of PO_2F_2 groups and stretching vibrations modes of LiO_4 groups. In fact, the overall spectrum of LiPO_2F_2 agrees favourably with the spectra of other metal difluorophosphates.¹⁷ Therefore, these results further confirm the rationality of X-ray single crystal structural analysis.

The thermal behaviour of LiPO_2F_2 was examined by thermal gravimetric (TG) and differential scanning calorimetry (DSC) technique. The result indicates that the stability of LiPO_2F_2 is below 350 °C. As shown in Figure 4a, a slow weight loss process could be observed on the TG curve between RT to 350 °C, which is probably caused by the hygroscopy of as-synthesized powder sample and release of H_2O thereof. From powder XRD patterns of LiPO_2F_2 at different temperature (Figure 4b), we may safely draw the conclusion that the peak observed around 381 °C on the DSC curve is an endothermic decomposition peak. The TG curve shows that the weight loss undergoes two steps in the range of 350–500 °C, resulting in a total weight loss of about 46%, which is attributed to the decomposition of LiPO_2F_2 . The first step points to the loss $\text{POF}_3(\text{g})$ and the residual products are mainly lithium metaphosphate $\text{LiPO}_3(\text{s})$ and $\text{LiF}(\text{s})$. The second step points again to the loss $\text{POF}_3(\text{g})$ and the residual products are $\text{Li}_4\text{P}_2\text{O}_7(\text{s})$ and $\text{LiF}(\text{s})$. The XRD patterns at 500 and 600 °C consist of $\text{Li}_4\text{P}_2\text{O}_7(\text{s})$ and $\text{Li}_3\text{PO}_4(\text{s})$, respectively. Since the meta- and pyrophosphates show far higher thermal stabilities, the sequence of formation of LiPO_3 , $\text{Li}_4\text{P}_2\text{O}_7$, and Li_3PO_4 with rising temperature is not just thermal release of $\text{P}_4\text{O}_{10}(\text{g})$ in this temperature range.¹⁸ Thus, additional support for the very stable gaseous molecule POF_3 is provided. Thermal decompositions of LiPO_2F_2 are analysed in detail in the ESI.

Additionally, we investigated the electronic structures of LiPO_2F_2 based on the density functional theory (DFT) (Figures S11 and S12, ESI).¹⁹ The title compound has an indirect band gap of 7.69 eV (HSE06) using the PWmat code,²⁰ which is one of the largest in alkali and alkaline earth metal fluorophosphates according to our previous work.^{4d} The ultraviolet–visible–near-infrared transmittance spectrum shows a cut-off edge less than 180 nm (Figure S13, ESI), which further demonstrates that LiPO_2F_2 has a wide ultraviolet transmittance window comparable to recently reported oxyfluoride deep-ultraviolet optical crystals, such as $\text{LiB}_6\text{O}_9\text{F}$,²¹ $\text{Li}_2\text{B}_6\text{O}_9\text{F}_2$,²² $\text{NH}_4\text{B}_4\text{O}_6\text{F}$,^{4c} $\gamma\text{-Be}_2\text{BO}_3\text{F}$,²³ $\text{BaB}_4\text{O}_6\text{F}_2$,²⁴ $\text{PbB}_5\text{O}_8\text{F}$,²⁵ $(\text{NH}_4)_2\text{PO}_3\text{F}$,^{4d} and $\text{K}_4\text{Si}_3\text{P}_2\text{O}_7\text{F}_{12}$.²⁶ The projected densities of states reveal that the valence band (VB) maximum is dominated by O-2p orbital, while the conduction band (CB) is formed primarily by the hybridization orbitals of P, O, Li atoms. Namely, the states on both sides of the band gap are mainly composed of the orbitals from P/Li–O bonds in LiPO_2F_2 . The F-2p orbital in LiPO_2F_2 exhibits quite large hybridization with the orbitals on the neighbour ions, which decreases the energy bandwidth of the VB and enlarges the band gap of LiPO_2F_2 . Therefore, the absorption edge of fluorophosphates, especially for

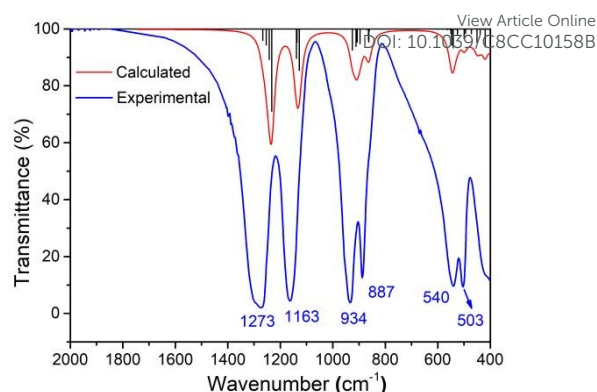


Figure 3. The spectra of as-synthesized LiPO_2F_2 . The red curve and black bars denote band positions calculated by DFT.¹⁹

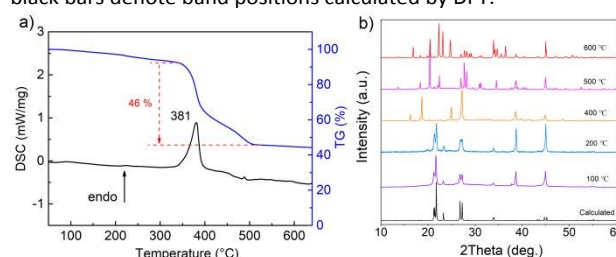


Figure 4. a) The TG-DSC curves of as-synthesized samples. The TG curve (blue solid line) shows two steps weight loss process in the temperature range of 350–500 °C. From the DSC curve (black solid line), a remarkable endothermic peak is observed at about 381 °C during the heating process. b) Powder XRD patterns of LiPO_2F_2 : calculated one, annealed at 100, 200, 400, 500 and 600 °C for 10 h, respectively. LiPO_2F_2 decomposes at 381 °C, and the residual products are mainly LiPO_3 (PDF# 26-1177) and LiF (PDF# 04-0857) at 400 °C, $\text{Li}_4\text{P}_2\text{O}_7$ (PDF# 13-0440) and LiF (PDF# 04-0857) at 500 °C, and Li_3PO_4 (PDF# 15-0760) and $\text{Li}_4\text{P}_2\text{O}_7$ (PDF# 13-0440) at 600 °C.

difluorophosphates, is blue-shifted compared with those of orthophosphates, which was also confirmed by the DFT calculations.^{4d} In addition, all O atoms in LiPO_2F_2 bridge three neighbouring P/Li atoms, which is beneficial for large band gap of LiPO_2F_2 . In addition, the calculated birefringence for LiPO_2F_2 is about 0.013 @1064 nm (Figure S14, ESI), which is smaller than those of other alkali metal difluorophosphates but larger than alkali or alkaline earth metal orthophosphates. From the insight of structure–property relationships, partial substitution of oxygen by fluorine in the PO_4 group results in the obvious anisotropy in both LUMO and HOMO. Therefore, the oxyfluoride PO_2F_2 groups have larger optical anisotropy than the PO_4 groups, as a result, difluorophosphates are more likely to produce larger birefringence than orthophosphates.

In summary, the first lithium difluorophosphate LiPO_2F_2 was synthesized under hydrothermal conditions and characterized by single-crystal XRD analysis, elemental analysis, IR spectra, and TG-DSC analysis. The structure is built up by isolated PO_2F_2 tetrahedra and interlaced 1D $[\text{LiO}_2]^{3-}$ straight chains forming a microporous 3D architecture. In addition, optical characterizations and theoretical analysis indicate that LiPO_2F_2 has a wide deep-ultraviolet transmittance window and large birefringence in comparison with orthophosphates owing to the unique oxyfluoride PO_2F_2 species. The BET(N_2) surface area of LiPO_2F_2 crystals are comparable to that of P25 TiO_2 nanoparticles, a commercial catalyst under ultraviolet light

irradiation. Considering the obvious advantages, we believe that difluorophosphates will provide an innovative avenue to get new materials with excellent functional properties in future.

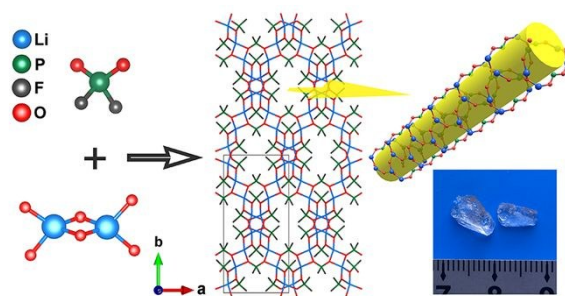
This work is supported by the National Natural Science Foundation of China (Grant Nos. 61835014, 51425206, 51602341, 91622107), the West Light Foundation of the CAS (Grant No. 2015-XBQN-B-11), the Natural Science Foundation of Xinjiang (Grant No. 2016D01B061), the National Key Research Project (Grant No. 2016YFB0402104), Xinjiang Key Research and Development Program (Grant No. 2016B02021), Key Research Project of Frontier Science of CAS (Grant No. QYZDB-SSWJSC049) and Shanghai Cooperation Organization Science and Technology Partnership Program (Grant No. 2017E01013).

Conflicts of interest

There are no conflicts to declare.

Notes and references

- (a) G. L. Clark and A. P. Tai, *Science*, 1948, **107**, 505-505; (b) Y. J. Fang, J. X. Zhang, L. F. Xiao, X. P. Ai, Y. L. Cao and H. X. Yang, *Adv. Sci.*, 2017, **4**, 1600392; (c) P. H. Abelson, *Science*, 1999, **283**, 2015-2015; (d) J. W. Qiao, L. X. Ning, M. S. Molokeev, Y.-C. Chuang, Q. L. Liu and Z. G. Xia, *J. Am. Chem. Soc.*, 2018, **140**, 9730-9736; (e) Y. X. Ma, Y. P. Gong, C. I. Hu, J. G. Mao and F. Kong, *J. Solid State Chem.*, 2018, **262**, 320-326; (f) D. Schildhammer, G. Fuhrmann, L. L. Petschnig, K. Wurst, D. Vitzthum, M. Seibald, H. Schottenberger and H. Huppertz, *Inorg. Chem.*, 2017, **56**, 2736-2741; (g) H. W. Yu, W. G. Zhang, J. Young, J. M. Rondinelli and P. S. Halasyamani, *Adv. Mater.*, 2015, **27**, 7380-7385; (h) A. Choudhury, S. Natarajan and C. N. R. Rao, *Chem. Commun.*, 1999, **0**, 1305-1306.
- (a) H. A. Prescott, S. I. Troyanov and E. Kemnitz, *Z. Kristallogr. - Cryst. Mater.*, 2000, **215**, 240-245; (b) H. A. Prescott, S. I. Troyanov, M. Feist and E. Kemnitz, *Z. Anorg. Allg. Chem.*, 2002, **628**, 1749-1755. (c) S. G. Jantz, L. van Wüllen, A. Fischer, E. Libowitzky, E. J. Baran, M. Weil and H. A. Höpfe, *Eur. J. Inorg. Chem.*, 2016, **2016**, 1121-1128; (d) K. Chihara, A. Katogi, K. Kubota and S. Komaba, *Chem. Commun.*, 2017, **53**, 5208-5211; (e) C. M. Julien, A. Mauger and H. Groult, in *Advanced Fluoride-Based Materials for Energy Conversion*, eds. T. Nakajima and H. Groult, Elsevier, 2015, pp. 77-101; (f) L. Li, Y. L. Xu, X. F. Sun, R. Chang, Y. Zhang, X. N. Zhang and J. Li, *Adv. Energy. Mater.*, 2018, **8**, 1801064; (g) H. Kim, D.-H. Seo, M. Bianchini, R. J. Clément, H. Kim, J. C. Kim, Y. Tian, T. Shi, W.-S. Yoon and G. Ceder, *Adv. Energy. Mater.*, 2018, **8**, 1801591.
- J. Durand, L. Cot and J. L. Galigne, *Acta Crystallogr. B.*, 1974, **30**, 1565-1569.
- (a) B. B. Zhang, G. Q. Shi, Z. H. Yang, F. F. Zhang and S. L. Pan, *Angew. Chem. Int. Ed.*, 2017, **56**, 3916-3919; (b) G. P. Han, Y. Wang, Z. B. Bing and S. L. Pan, *Chem. - Eur. J.*, 2018, **24**, 17638-17650; (c) G. Q. Shi, Y. Wang, F. F. Zhang, B. B. Zhang, Z. H. Yang, X. L. Hou, S. L. Pan and K. R. Poeppelmeier, *J. Am. Chem. Soc.*, 2017, **139**, 10645-10648; (d) B. B. Zhang, G. P. Han, Y. Wang, X. L. Chen, Z. H. Yang and S. L. Pan, *Chem. Mater.*, 2018, **30**, 5397-5403; (e) S. G. Jantz, M. Dialer, L. Bayarjargal, B. Winkler, L. van Wüllen, F. Pielhofer, J. Brgoch, R. Weihrich and H. A. Höpfe, *Adv. Opt. Mater.*, 2018, **6**, 1800497; (f) Y. Wang, B. B. Zhang, Z. H. Yang and S. L. Pan, *Angew. Chem. Int. Ed.*, 2018, **57**, 2172-2176. DOI: 10.1039/C8CC10158B
- (a) L. Ma, L. Ellis, S. L. Glazier, X. W. Ma, Q. Q. Liu, J. Li and J. R. Dahn, *J. Electrochem. Soc.*, 2018, **165**, A891-A899; (b) Q. Q. Liu, L. Ma, C. Y. Du and J. R. Dahn, *Electrochim. Acta* 2018, **263**, 237-248; (c) W. M. Zhao, G. R. Zheng, M. Lin, W. G. Zhao, D. J. Li, X. Y. Guan, Y. J. Ji, G. F. Ortiz and Y. Yang, *J. Power Sources* 2018, **380**, 149-157; (d) *Republic of Korea Pat.*, EP2881366A1, 2013.
- R. W. Harrison, R. C. Thompson and J. Trotter, *J. Chem. Soc. A*, 1966, **0**, 1775-1780.
- W. Granier, J. Durand, L. Cot and J. L. Galigne, *Acta Crystallogr. B.*, 1975, **31**, 2506-2507.
- J. Trotter and S. H. Whitlow, *J. Chem. Soc. A*, 1967, **0**, 1383-1386.
- R. Harrison and J. Trotter, *J. Chem. Soc. A*, 1969, **0**, 1783-1787.
- (a) N. E. Brese and M. O'Keeffe, *Acta Crystallogr. B.*, 1991, **47**, 192-197; (b) I. D. Brown and D. Altermatt, *Acta Crystallogr. B.*, 1985, **41**, 244-247; (c) R. Hoppe, S. Voigt, H. Glaum, J. Kissel, H. P. Müller and K. Bernet, *J. Less. Common. Met.*, 1989, **156**, 105-122.
- R. J. Gillespie and R. S. Nyholm, *Q. Rev. Chem. Soc.*, 1957, **11**, 339-380.
- K. M. Ok, *Acc. Chem. Res.*, 2016, **49**, 2774-2785.
- (a) W. A. Henderson and N. R. Brooks, *Inorg. Chem.*, 2003, **42**, 4522-4524; (b) M. S. Wickleder, *Z. Anorg. Allg. Chem.*, 2003, **629**, 1466-1468.
- Z. Zak and M. Kosicka, *Acta Crystallogr. B.*, 1978, **34**, 38-40.
- S. T. Wilson, B. M. Lok, C. A. Messina, T. R. Cannan and E. M. Flanigen, *J. Am. Chem. Soc.*, 1982, **104**, 1146-1147.
- X. Y. Fan, L. Zang, M. Zhang, H. S. Qiu, Z. Wang, J. Yin, H. Z. Jia, S. L. Pan and C. Y. Wang, *Chem. Mater.*, 2014, **26**, 3169-3174.
- (a) R. Thompson and W. Reed, *Inorg. Nucl. Chem. Lett.*, 1969, **5**, 581-585; (b) T. H. Tan, University of British Columbia, 1970.
- A. Daidouh, M. L. Veiga, C. Pico and M. Martinez-Ripoll, *Acta Crystallogr.*, 1997, **C53**, 167-169.
- S. J. Clark, M. D. Segall, C. J. Pickard, P. J. Hasnip, M. I. Probert, K. Refson and M. C. Payne, *Z. Kristallogr. - Cryst. Mater.*, 2005, **220**, 567-570.
- (a) W. Jia, Z. Cao, L. Wang, J. Fu, X. Chi, W. Gao and L.-W. Wang, *Comput. Phys. Commun.*, 2013, **184**, 9-18; (b) W. Jia, J. Fu, Z. Cao, L. Wang, X. Chi, W. Gao and L.-W. Wang, *J. Comput. Phys.*, 2013, **251**, 102-115.
- (a) G. Cakmak, J. Nuss and M. Jansen, *Z. Anorg. Allg. Chem.*, 2009, **635**, 631-636; (b) B. Andriyevsky, K. Doll, G. Cakmak, M. Jansen, A. Niemer and K. Betzler, *Phys. Rev. B*, 2011, **84**, 125112.
- (a) T. Pilz and M. Jansen, *Z. Anorg. Allg. Chem.*, 2011, **637**, 2148-2152; (b) B. Andriyevsky, T. Pilz, J. Yeon, P. S. Halasyamani, K. Doll and M. Jansen, *J. Phys. Chem. Solids* 2013, **74**, 616-623.
- G. Peng, N. Ye, Z. S. Lin, L. Kang, S. L. Pan, M. Zhang, C. S. Lin, X. F. Long, M. Luo, Y. Chen, Y. H. Tang, F. Xu and T. Yan, *Angew. Chem. Int. Ed.*, 2018, **57**, 8968-8972.
- S. G. Jantz, F. Pielhofer, L. van Wüllen, R. Weihrich, M. J. Schäfer and H. A. Höpfe, *Chem. - Eur. J.*, 2018, **24**, 443-450.
- M. Mutailipu, M. Zhang, B. B. Zhang, Z. H. Yang and S. L. Pan, *Chem. Commun.*, 2018, **54**, 6308-6311.
- G. P. Han, B.-H. Lei, Z. H. Yang, Y. Wang and S. L. Pan, *Angew. Chem. Int. Ed.*, 2018, **57**, 9828-9832.



View Article Online
DOI: 10.1039/C8CC10158B

The first lithium difluorophosphate LiPO_2F_2 with a unique microporous architecture and improved optical properties was synthesized and characterized.